

FIELD STUDY AND BIDIMENSIONAL NUMERICAL SIMULATION OF RUNOUT AND DEPOSITION OF LA MAROGNA ROCKSLIDE (VICENZA, ITALY)

PIA ROSELLA TECCA^(*), RINALDO GENEVOIS^(**),
ANDREA MARIA DEGANUTTI^(*) & MARCO DAL PRÀ^(***)

^(*) CNR - IRPI - Padua, Italy

^(**) Università degli Studi di Padova - Dipartimento di Geoscienze - Padua, Italy

^(***) Professional geologist

ABSTRACT

The study of ancient major rock slope instabilities may help in the detection of the conditions leading to their development, so that consequences and possible prevention and mitigation actions can be envisaged.

In this paper, numerical studies have been carried out to recognize the behavior of a rock slope and the kinematics of a rock slide/avalanche in the north-eastern Italian Alps. The “La Marogna” rock avalanche, in the Vicenza Province (Venetian Pre-Alps, North-Eastern Italy), with a volume of about $17 \times 10^6 \text{ m}^3$, still partially dams the narrow valley of the Astico River. Geomorphological investigations highlight that the whole rock avalanche mass is formed by two distinct overlapping bodies and that apparent poor stability conditions characterize the slope above the present main scarp.

In order to get indications about triggering factors and present stability conditions, a representative engineering geological model has been built and analyses of the triggering conditions have been performed using the bi-dimensional continuum (FLAC) and discontinuum (UDEC) codes UDEC on the re-constructed original slope profile. Different situations have been simulated for gaining a better understanding of the effect of static and dynamic loads on the modeled rock slope.

The numerical results indicate that the effect of a contemporary dynamic loading and joint friction decrease results in the instability of a rock mass limited at its bottom by both bedding and a pre-existing discontinuity.

KEY WORDS: rock slide/avalanche, FLAC, UDEC, dynamic analysis

INTRODUCTION

Catastrophic rockslides, damming valleys with a subsequent dam failure, have always occurred worldwide. The relevance of this process as a natural hazard stresses the need for a more complete knowledge of both the triggering mechanism and the prediction of life span of rockslide dams.

Rock slope stability depends on the strength of the rocks, the geometrical and strength characteristics of the discontinuities (roughness, wall strength and persistence) and on the weathering action on the intact rock and discontinuities.

Since a rock mass is not a continuum, its behavior is dominated by discontinuities such as faults, joints and bedding planes. In general, because the presence or absence of discontinuities has a great influence on the stability of rock slopes, their behavior plays a critical role in a stability evaluation.

Understanding the factors leading to the development of rock slopes instability and failure has far reaching implications for the safe development of both inhabited alpine valleys and engineering projects.

In this paper, the finite difference (FLAC) and the distinct element (UDEC) codes have been used to model the evolution of a rock slope thought to have failed in response to a seismic shaking. The numerical simulation is aimed, then, to explain whether the

rock slope collapse, with the typical features of a rock avalanche (“La Marogna” rock avalanche), was triggered by the earthquake occurred on 1117.01.03 (10 IX MCS, M 7.0) (MADDALENA, 1906; GUIDOBONI *et alii*, 2005) or the sliding took place just during the deglaciation most-unstable situation.

“La Marogna” rock avalanche, located in the Astico Valley (Venetian Pre Alps, North-Eastern Italy), has been analyzed both in static and dynamic conditions to investigate the trigger mechanism and providing the possibility to evaluate the stability conditions of the present slope. The geological and structural setting of the area has been investigated by ZAMPIERI &

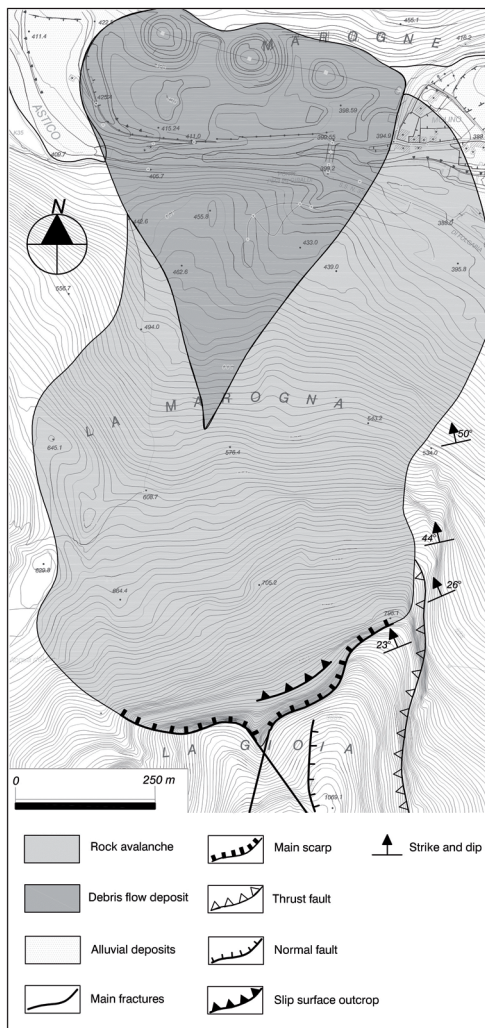


Fig. 1 - Geological schematic map of the “La Marogna” rock avalanche

ADAMI (2013, this volume) in order to identify large-scale instability structures that might have induced the mass movement.

GEOLOGY AND GEOMORPHOLOGY

“La Marogna” rock avalanche (Fig. 1), detached from the steep-sided right slope of the Astico River Valley, with a local NW-SE trend. The slope is composed of the Mesozoic formation of “Dolomia Principale” characterized by well-bedded carbonates. This slope belongs to the northern limb of an anticline fold so that the bedding dip, NNW trending, increases progressively from 20°-25° at the slope top to about 50° at the bottom (Dal Prà, 1992). The fold limb is affected in the higher part of the slope by a normal fault, dipping 70° ENE, by vertical persistent tectonic lineaments and by some trenches not directly correlated to the instability phenomenon (ZAMPIERI & ADAMI, 2013; this volume). The upper part of the slope is characterized by a sub-vertical scarp, about 600 m long and 160-180 m high.

The rock avalanche run along the anticline limb and the sliding surface is well exposed at the base of the main scarp, where the beds dip 30°-35° as a mean (Fig. 2).

The anticlinal structure is well exposed on the 300 m high East facing cliff (Fig. 2), where it is also possible to note the presence of a NNW dipping thrust (“b” in figure 2) with a “stair case” geometry: steep reverse fault tracts in stiff layers connect flat tracts sub-parallel to the bedding.

It is worthwhile to note that the lower flat tract, located at the transition between the lower thinner and the upper thicker layers of the “Dolomia Principale”,



Fig. 2 - East facing cliff. a : anticlinal structure ; b : main thrust ; c : minor thrust's element ; d : dip of the outcropping sliding surface

represents the up-hill prosecution of the bedding visible just down-hill (Fig. 2) (ZAMPIERI & ADAMI, 2013, in this volume). A secondary shorter tectonic structure, indicated with “c” in Fig. 2, is present. Three main sub-vertical joint systems cross the rock mass, trending approximately N310°-320°, N230° and N260°-270°.

The whole rock avalanche deposit is formed by two distinct overlapping bodies: the former develops from the base of the main scarp to the valley bottom. It is covered by a fan-shaped body rising up the opposite slope for about 40 m, due to a later process with the features of a rock/debris flow. The deposits dammed the Astico River, and the resulting lake should have drained in a very short time, since no lacustrine sediments have been found upstream. The deposit is formed by sands, gravels and pebbles with blocks from 1 to several tens m³ and no remarkable granulometric differences are shown by the two bodies. Two C¹⁴ datings of timbers, collected at the base of the landslide deposit, are consistent with the 1117.01.03 earthquake (BARBIERI *et alii*, 2007) to which the rock avalanche is attributed.

The total volume of the landslide deposit results to be in the order of 16.9x10⁶ m³. The volume of the first phenomenon has been calculated in about 5.5x10⁶ m³, while the later one in about 11.4x10⁶ m³. Assuming a bulking coefficient of 0.30, the initial collapsed rock volume is about 13x10⁶ m³, split between the two slides respectively in 4.2x10⁶ m³ and 8.8x10⁶ m³.

NUMERICAL MODELING

Numerical models, both continuum and discontinuum, represent an alternative effective method to compute the interaction between different materials, site geometry and wave propagation in case of seismic inputs (BOUSSOU, 2012; BOZZANO *et alii*, 2004).

In the equivalent continuum models for jointed rock masses (SINGH, 1973a,b; GOODMAN, 1976; GERRARD, 1982), usually referred to as compliant joint models or ubiquitous joint models, the original discontinuous material is replaced by a hypothetical continuous material using a homogenization technique. When coupled with a discontinuum modeling, two-dimensional continuum modeling may be used to preliminarily examine stress distribution and evolution, possible phases of stress-induced progressive failure, and plastic yielding within the rock mass. As such, a preliminary set of 2-D models were run using the con-

tinuum code FLAC (ITASCA, 2012) mainly investigating strength degradation leading to failure and calibrating strength parameters.

Continuum models, however, do not give reliable information on internal displacement field and discontinuity-controlled failures. Discontinuum modeling approach explicitly simulates the geological structure treating the problem domain as an assemblage of independent units, corresponding to blocks formed by the intersection of joints (LORIG *et alii*, 1991). The basic difference with continuum-based methods is that contacts between blocks are continuously changing with the deformation process. A more realistic response can be, then, modeled and the specific failure mechanism, controlled by pre-defined discontinuities, may be captured.

Discontinuum modeling, such as the distinct element 2D-code UDEC (ITASCA, 2011) probably constitutes the most commonly applied numerical approach to rock slope analysis.

ESTIMATION OF ROCK MASS AND JOINTS PROPERTIES

A number of in situ tests and some laboratory tests have been performed to set representative mean values of the properties of rocks and discontinuities. Uniaxial compressive tests were conducted in laboratory, while joint parameters JRC0 and JCS0 were estimated by field Barton roughness profiles and Schmidt hammer tests in 8 and 140 kPa respectively. Values of the rock mass strength and deformation parameters were obtained using the RocLab program (HOEK, 2007). Mechanical properties values of rocks and intact and weathered rock masses are shown in Tab. 1.

Observed discontinuities are predominantly unaltered. Sub-vertical joints are mostly rough while bedding planes are prevalingly undulating and less rough. The residual friction angle (ϕ_r) has been estimated respectively to 30° and 28°. Approximate stiffness values of discontinuities have been back-calculated from data on deformability of both intact rock and rock mass (ITASCA, 2011). The scale corrections for in situ block sizes have been derived using the corrections proposed by BARTON & BANDIS (1990), obtaining corrected JRC and JCS values, respectively 6 and 65 MPa. Shear (G) and bulk (K) moduli were calculated on the basis of rock mass deformation modulus and a Poisson coefficient of 0.23.

| Material | ρ (kg/m ³) | σ_{ci} (KPa) | E (KPa) | c (KPa) | ϕ (°) | t (KPa) |
|---------------------|--------------------------------|------------------------|------------|------------|---------------|------------|
| Intact rock | 2.7e3 | 1.25e5 | 6.25e7 | 6.2e3 | 53.6 | -2.3e3 |
| Rock mass | 2.6e3 | 7.5e3 | 1.25e7 | 1.7e3 | 45.4 | -2.9e2 |
| Weathered Rock mass | 2.6e3 | 2.4e3 | 4.6e6 | 1.1e3 | 38.2 | -1.2e2 |

Tab. 1 - Initial strength parameters of rock and rock masses. ρ : density; σ_{ci} : uniaxial compressive strength; E: elastic modulus; c: cohesion; ϕ : friction angle; t: tensile strength

| Material | Model | ρ (g/m ³) | K (KPa) | G (KPa) | c (KPa) | j_c/j_{c_r} (KPa) | ϕ (°) | j_ϕ/j_{ϕ_r} (°) | t (KPa) | j_t/j_{t_r} (KPa) |
|-----------------|---------|-------------------------------|------------|------------|------------|------------------------|---------------|----------------------------|------------|------------------------|
| Rock mass | ub | 2.7e3 | 7.7e6 | 5.1e6 | 1.7e3 | 5e1/5e1 | 45 | 45/38 | -2.9e2 | -1e1/0 |
| Ice | Elastic | 0.92e3 | 6.9e6 | 3.6e6 | - | - | - | - | - | - |
| Collapsing mass | su | 2.7e3 | 2.8e6 | 1.9e6 | 1.7e3 | 5e1/1e1 | 38 | 38/28 | -3.4e2 | -1e1/0 |

Tab. 2 - Continuum stability analysis parameters and models

| Static and dynamic analyses | Material | Constitutive Model | ρ (kg/m ³) | K (KPa) | G (KPa) | c (KPa) | ϕ (°) | t (KPa) |
|-----------------------------|----------|--------------------|--------------------------------|------------|------------|------------|---------------|------------|
| | Rock | MC | 2.7e3 | 3.9e7 | 2.5e7 | 6.2e3 | 53.6 | -2.3e3 |
| | Ice | Elastic | 0.92e3 | 6.9e6 | 3.6e6 | - | - | - |

Tab. 3 - Rock material properties and models for discontinuum analyses

| | Static analysis | | | | | | | |
|-----------------------|--------------------|----------------|----------------|----------------|----------------|-----------------|-----------------|----------------|
| | Constitutive Model | JKN (KPa/m) | JKS (KPa/m) | j_c (KPa) | j_t (KPa) | j_ϕ (°) | Dip (°) | Spacing (m) |
| Subvertical joint set | MC | 13e6 | 5.3e6 | 5e1 | 5 | 42 | 80 | 50 - 80 |
| Bedding | MC | 7.7e6 | 3e6 | 2 | 1 | 38 | 20 - 50 | 40 |
| Thrust surface | CS | 7.7e6 | 3e6 | 0 | 0 | 38 | 33 | - |
| | Dynamic analysis | | | | | | | |
| | Constitutive Model | JKN (KPa/m) | JKS (KPa/m) | j_c (KPa) | j_t (KPa) | j_ϕ (°) | j_ϕ (°) | j_r (m) |
| Subvertical joint set | CS | 13e9 | 5.3e6 | 5e1 | 5 | 42 | - | - |
| Bedding | CY | 7.7e6 | 3e6 | 2 | 0 | 38 | 28 | 0.02 |
| Thrust surface | CY | 7.7e6 | 3e6 | 0 | 0 | 38 | 28 | 0.02 |

Tab. 4 - Joints properties and models

The mechanical properties of rocks, ice and joints, used in the static and dynamic discontinuum modeling, are listed in Tables 2, 3 and 4.

STABILITY ANALYSES

Both continuum and discontinuum stability analyses have been carried out as follows: 1) the original slope has been re-drawn on the basis of the surrounding morphology and the calculated landslide volume; 2) the stresses have been initialized considering the existence of a 800 m high glacier progressively reducing its height; 3) in continuum modeling, ubiquitous-joint and strain-hardening/softening ubiquitous-joint models have been considered; 4) in discontinuum modeling, Mohr-Coulomb, Coulomb slip and continuously yielding models have been considered; 5) seismic loading has been

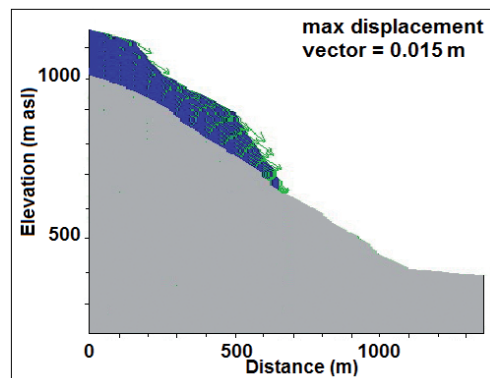


Fig. 3 - Static continuum analysis: displacement vectors in dry conditions and constitutive models. Ubiquitous joint model: grey; Strain softening ubiquitous joint model: blue

simulated applying a sinusoidal stress wave (continuum model) or a sinusoidal velocity wave (discontinuum model), whose frequencies and intensities have been selected on the basis of the Italian Seismic Risk Maps (INGV, 2007).

CONTINUUM MODELING

Considering the observed relationship between rock mass anticlinal structure and sliding surface, continuum numerical methods have been preferred to preliminarily simulate the mass structure behavior subjected to quasi-static or dynamic loading.

Two-dimensional modeling was carried out using the finite-element code FLAC 7.0 (ITASCA, 2012), that is able to efficiently model progressive and time-dependent failure mechanisms. The model incorporated 837 quadrilateral elements and the grid has been drawn to fit the existing anticlinal structure. An elasto-plastic constitutive criterion has been assigned to the slope materials assuming a Mohr-Coulomb yield criterion; stresses have been initialized assuming a gravity loading and an elastic homogeneous isotropic rock mass. Before the removal of the glacier, an ubiquitous-joint model and a strain-hardening/softening ubiquitous-joint model have been assigned respectively to the base rock mass and to the rock collapsing mass, to take account of both material anisotropy and the continuously changing dip of bedding (Fig. 3).

Strength parameters values have been initially set to those for intact rocks (Tab. 1). The progressive degradation of rock mass strength with stress variation and time has been simulated by gradually decreasing the values of rock properties up to reaching the calculated properties values of weathered rock mass (Tab. 2).

In dry conditions, the slope is completely stable: small displacements are essentially restricted to the steeper parts of the reconstructed slope (Fig. 3). In case of the presence of a groundwater with a maximum height of 10 m over the indicated shear surface, the rock slope is still stable but, at the base and at the top of the potentially collapsing mass, finite slips along the ubiquitous joints develop (Fig. 4). In conclusion, the examination of the 2-D finite-element results in static conditions shows that a condition of instability cannot be reached, even considering the presence of a perched water table in the potentially collapsing mass.

In order to investigate the triggering mechanism

and the plausibility of a slope collapse in conjunction with a seismic event, continuum analysis have been carried out in dynamic conditions.

On the basis of the macroseismic field (SERVA, 1990), the 03/01/1117 earthquake intensity has been estimated in VIII-IX MCS, that is a magnitude of $M=6-7$, and the corresponding PGA (Peak Ground Acceleration) considered equal at least to $0.32g$ with frequencies from 2 to 5 Hz. However, the Italian Risk Map (INGV, 2007) shows, in the same area and for an exceedence probability of 1% in 50 years, a PGA of $0.25g$. The analyses have been, then, performed considering two values of the maximum acceleration $a_{max} : 0.25g$ and $0.32g$. Using existing empirical correlations, the duration of the seismic loading has been evaluated in a minimum of 8 seconds.

The dynamic input has been provided applying a sinusoidal shear wave to the base of the model, free to propagate upwards and, for simplicity, isotropic conditions have been assumed. The input variables for dynamic analysis have been calculated from the expressions (BHASIN & KAYNIA, 2004; ITASCA, 2012):

$$V_{max} = \frac{a_{max}}{2\pi f}; \quad V_s = \sqrt{G/\rho}; \quad \tau = (V_s * \rho * V_{max})$$

where V_{max} is the ground motion velocity (m/s), $2\pi f$ the angular frequency, V_s the shear wave velocity (m/s) and τ the shear stress, doubled to compensate for viscous boundaries. The sinusoidal shear wave has been applied for different periods (8, 12, 24 s) representing cycles of motion from 16 to 120. Values of input seismic parameters are summarized in Tab. 5.

Examination of the results obtained with a dura-

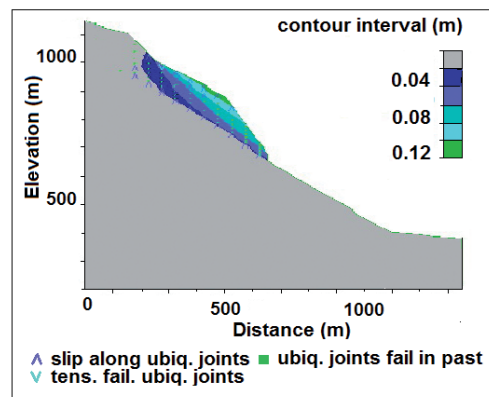


Fig. 4 - Static continuum analysis with a water table: horizontal displacements distribution and plasticity indicators

tion of 8 seconds (test n. 6) shows that (Fig. 5): i) maximum horizontal displacements, greater than 6.0 m in the steeper part of the slope, propagate towards the higher part of the slope, being maximum at the toe and approximately null at a distance of 550 m; ii) slips along ubiquitous joints are distributed in all the collapsing mass; iii) the upper end of the sliding mass is limited by zones at failure in tension. The instability condition is shown by the horizontal velocities progressively increasing with time, monitored at selected points on the shear surface (Fig. 6).

In conclusion, the dynamic simulation indicates that an earthquake with the characteristics of that occurred in 1117 A.D. might have triggered the "La Marogna" rock avalanche but, with continuum modeling, the shape of the collapsed mass does not completely reflect the present morphology of the slope: the slip surface follows the local maximum rock strata dip, but the simulated sliding mass extends far beyond the location of the present landslide scarp. In any case, the examined rock slope seems to be more sensitive to the seismic frequency than to the seismic acceleration, at least considering a dynamic time of 8 seconds.

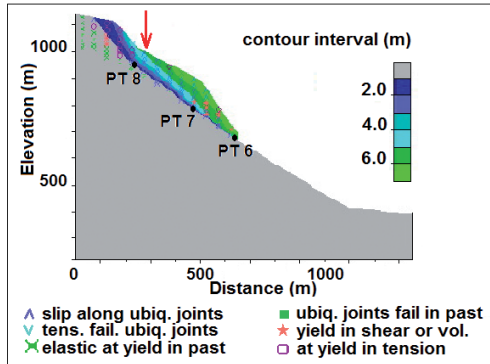


Fig. 5 - *x*-displacements contours, monitored points PT and plasticity indicators for dynamic conditions ($a=0.32g$, $f=5$ Hz, duration 8 s, $\tau=587$ KPa). Location of the present landslide scarp (red arrow)

DISCONTINUUM STABILITY ANALYSES

In order to investigate the control of pre-defined discontinuities on slope failure, discontinuum stability analyses, in both static and dynamic conditions, were carried out using the two-dimensional distinct element code UDEC (ZHANG *et alii*, 1997).

The geometry of the joints has been generated according to statistical data collected by field measure-

| Test n. | a_{max} (g) | Frequency (Hz) | Duration (s) | V_{max} (m/s) | τ (KPa) |
|---------|---------------|----------------|--------------|-----------------|--------------|
| 1 | 0.25 | 2 | 8-12-24 | 0.020 | 376 |
| 2 | 0.32 | 2 | 8-12-24 | 0.025 | 470 |
| 3 | 0.25 | 3 | 8-12-24 | 0.013 | 244 |
| 4 | 0.32 | 3 | 8-12-24 | 0.017 | 320 |
| 5 | 0.25 | 5 | 8-12-24 | 0.008 | 150 |
| 6 | 0.32 | 5 | 8-12-24 | 0.010 | 188 |

Tab. 5 - Seismic parameters used in continuum modeling dynamic analyses a_{max} : peak ground acceleration; V_{max} : ground motion velocity; τ : shear stress

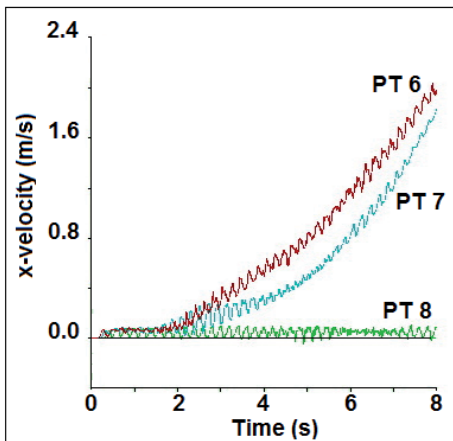


Fig. 6 - *x*-velocities vs dynamic time at monitored points PT 6, PT 7 and PT 8

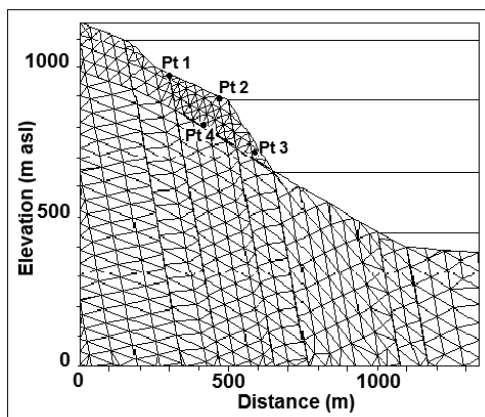


Fig. 7 - Discretization of the blocks into deformable finite-difference zones and location of the monitored points PT

ments. Basically, three sets of joints, that include the bedding planes and cross fractures, are represented in the model.

The dimension of blocks has been established considering that dynamic analyses will be carried out. In dynamic conditions, in fact, the mesh size is controlled by the shortest wavelength of input fluctuation (ITASCA, 2011). Thus the maximum size of the grid Δl should be less than $(1/10 \div 1/8)$ the shortest wavelength of seismic wave λ . The highest frequency of the input wave f_{max} , which cannot make waveform distorted, can be written as:

$$f_{max} = V_s / 10\Delta l$$

where V_s is the shear wave velocity (m/s). The grid size of the discrete elements has been selected considering that the maximum input frequency of considered dynamic loads is 5 Hz.

The slope was divided into blocks and the interior region was discretized into 722 fully deformable triangular elements. The base is assumed to be flexible but the boundary is fixed in the y-direction. Figure 7 displays the model of the jointed slope and the ice sheets.

The analyses have been performed considering: i) fully persistent and interconnected discontinuities; ii) presence of a persistent tectonic discontinuity (“b” in Fig. 2) and a shorter and steeper discontinuity (“c” in Fig. 2); iii) material properties deriving from the continuum modeling analyses; iv) glaciation and deglaciation processes have been modeled after the application of the rock mass properties values (Tab. 4, Static analysis), in order to consider the modification of stresses in the transition from glacial to non-glacial conditions (IVERSON, 2012); v) in static analysis, Mohr-Coulomb constitutive model for rock material, bedding and sub-vertical joints and Coulomb Slip model for the tectonic discontinuities; vi) in dynamic analysis, Coulomb Slip

model for sub-vertical joints and Continuously Yielding model for bedding and tectonic discontinuities.

UDEC modeling has been performed through the following steps: i) the model has been elastically equilibrated under the gravity force with the obtained rock parameters values (Tab. 3); ii) the load due to ice sheets has been applied to the model and later removed in successive stages; iii) static and dynamic analyses have been performed with rock and discontinuities properties and models shown in Tables 3 and 4 respectively.

In the static condition the slope resulted to be stable considering both the persistent tectonic discontinuity (“b” in Fig. 2) and the shorter one (“c” in Fig. 2): computed horizontal displacement rate induced by ice sheets removal is null. The results diverge only as regards the distribution of the calculated displacements: in the former case they develop over the persistent tectonic discontinuity up to the top of the modeled slope, while in the last case, they are limited upslope in correspondence of the present location of the landslide crown (Fig. 8), representing in a better way the future collapsing mass.

The dynamic analysis has been performed applying to the base of the model a S-wave with a peak amplitude of 0.08, 0.1, 0.13, 0.16 m/s (acceleration of 0.25 g and 0.32 g) at 3 and 5 Hz for 24 and 40 cycles (duration of dynamic input of 8 seconds). Frequency, amplitude and accelerations values have been selected as those used in the continuum modeling dynamic analysis. Free-field boundaries are invoked along the left and right boundaries to absorb energy and no displacement is allowed in the x-direction along the lateral sides of the model. The Rayleigh damping ratio, which reproduces the energy losses in the natural system when subjected to dynamic loading, has been assumed to equal 2%.

Analyses have been performed starting with the initial static equilibrium condition of the slope. The seismic parameters for the dynamic analysis are displayed in Tab. 5.

The dynamic analysis of the slope featuring the longest tectonic discontinuity (“b” in Fig. 2), 60 seconds after the end of the dynamic input (test 2), shows that the slope is entirely unstable. However, the collapsing mass does not match the field observation: significant displacements involve also the upper part of the slope, beyond the present location of the landslide crown (Fig. 9).

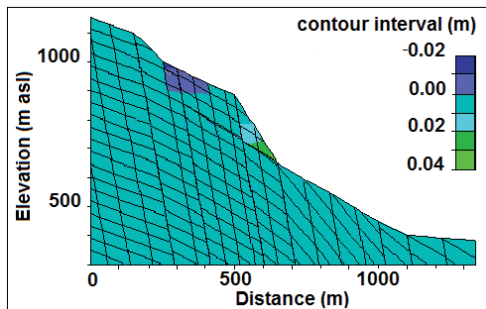


Fig. 8 - Static stability analysis

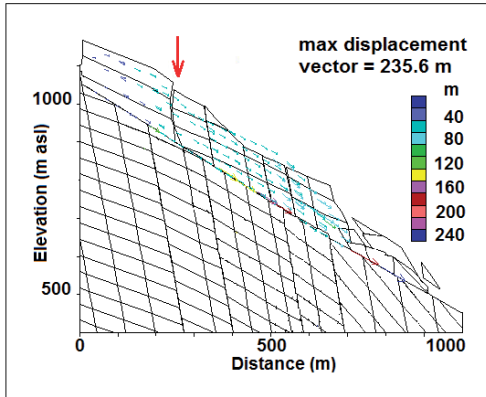


Fig. 9 - Block deformation 5-times amplified and displacement vectors 60 sec after the end of dynamic loading ($\alpha: 0.32g$; $f: 5\text{ Hz}$)

The analyses have been done again considering the observed shorter discontinuity (“c” in Fig. 2).

The sequence of displacements at different times after the end of the dynamic loading (Fig. 10) indicates the slope instability but, in this case, the collapsing mass matches rather well the present slope geometry. The displacement dynamics, highlighted also by the amplification of blocks deformation, shows that the collapsing mass is split in two main parts as indicated by the sub-vertical joint progressive aperture, the most upward part being characterized by a delayed dynamics.

However, after 60 s from the end of the seismic shaking, the two blocks move with the same velocity (monitored points PT 2 and PT 3, Fig. 11). It is also worthwhile to note the pulsating trend of the horizontal

velocities that could be the consequence of the variation of normal load and frictional resistance activation on the sliding surface and at the blocks contacts.

DISCUSSION AND CONCLUSIONS

This paper presents the numerical study of the “La Marogna” rockslide, probably earthquake triggered, based on geological observations, field data, and laboratory tests. In order to analyze the influence of geological and seismic factors on slope failure, numerical simulations were performed using both continuum (FLAC) and discontinuum (UDEC) bi-dimensional approaches.

The detailed geological investigation has shown that the sliding surface coincides partly with the dip of the existing anticlinal fold and, apparently, partly with a long thrust cutting the upper portion of the same anticline.

The initial estimate of the impact of geological setting (anticlinal structure and long thrusts) and geomechanical characteristics on slope stability was made under static conditions. Both continuum and discontinuum modeling revealed the stability of the slope with the strength parameters values obtained by field and laboratory tests and realistic water pressures on sliding surface.

However, simulation results do not match satisfyingly the morphology of the present slope: the real uphill extension of the collapsed rock mass may be simulated only considering the existing secondary tectonic discontinuity, shorter and more tilted than the more evident and long one. The discontinuum approach simulates effectively this discontinuity, showing that

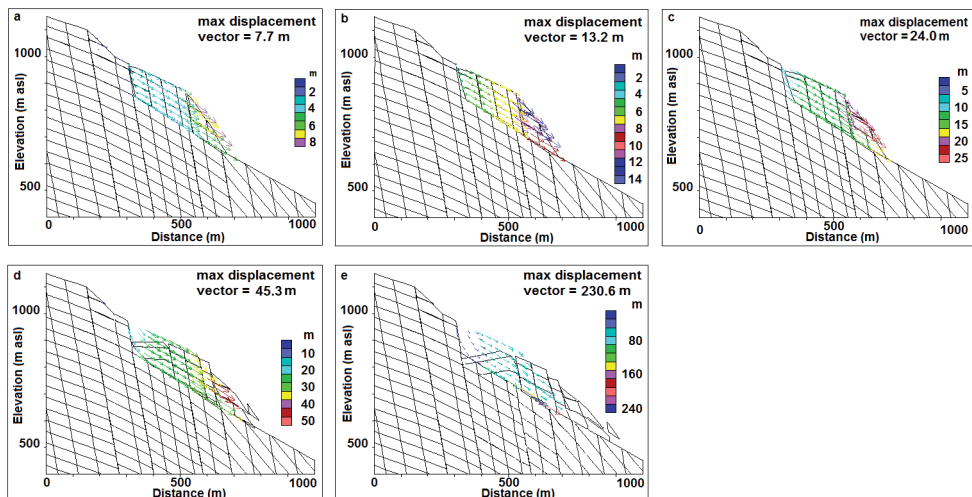


Fig. 10 - Sequence of block deformation 5-times amplified and displacement vectors in the unstable rock mass 0 sec (a), 5 sec (b), 10 sec (c), 30 sec (d) and 60 sec (e) after the end of dynamic loading

the rockslide detaches in correspondence of the present scarp and, so, stressing the necessity for accurate and detailed structural geology surveys in order to reproduce the real landslide formation mechanism.

Dynamic analyses, carried out considering historic data and seismic characteristic of the region, showed that the shear resistance of the controlling slip surface may be exceeded by the shaking-induced inertial forces due to, at least, a medium intensity earthquake, that is lower than that ($M=7.0$) of the 1117 A.D. earthquake. The duration of the seismic loading seems to be not so relevant as collapse may be modelled with a seismic shaking duration of only 8 s. In general terms, the slope collapse occurs for source frequencies in the range of those that may be attributed to this earthquake and large continuous post-seismic displacements develop with increasing velocities. Maximum horizontal velocities at the surface of the landslide body reach 0.6 m/s after 60 s from the end of the seismic loading (Fig.10) increasing, then, abruptly so that “La Marogna” rockslide may be categorized as a high-speed landslide.

For the studied slope height (160-180 m) and input frequencies (3 and 5 Hz) the ratio of slope height and input frequency is included between 0.13 and 0.26, that is generally considered critical for seismic amplification (DHAKAL, 2004).

The results of numerical analyses show that, in case of rock slopes, the discontinuum approach may be considered more reliable, but it requires more accurate and detailed field surveys that not always can be easily and completely obtained. Continuum approach is, on the other hand, useful in order to preliminarily simulate the mass structure behavior subjected to quasi-static or dynamic loading and analyze the corresponding stresses distribution.

However, while the triggering mechanism of the rockslide has been correctly reproduced, the dynamics is the main object of coming researches. As a matter of facts, the field observation indicates the presence of two different landslide deposits attributable to different processes, while the numerical simulation shows a unique sliding phenomenon. It should be highlighted, nevertheless, that the sequence of displacements following the seismic loading (Fig. 10) displays a rock mass that, before the general collapse (Fig. 10 e) is broken up in two parts with different dynamics: the smaller front part, where the reconstructed slope is steeper, moves earlier, while the larger rear one moves more

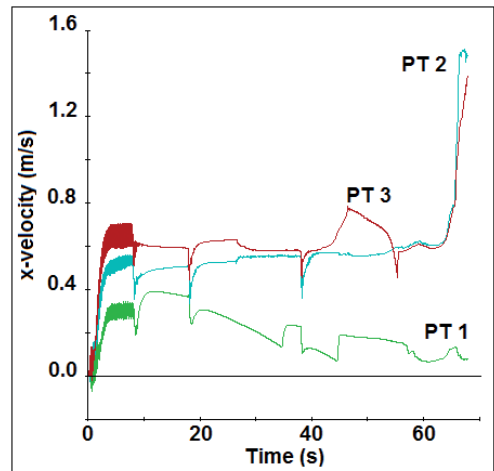


Fig. 11 - Test n. 2: time histories of horizontal velocities at monitored points PT 1, PT 2, PT 3. First 8 seconds refer to the seismic loading

slowly, separating in this way from the former one. This circumstance is confirmed by the different values and trend of the velocities registered at the surface ground monitored points (Fig. 11).

It is possible, then, to suppose that the earthquake triggered the front part of the rock mass that slid down as a rock avalanche and deteriorated the rear part that, however, remained on site. Only later this rock mass was destabilized probably by an increase of pore pressure due to heavy rain, so accounting for the fan shape of its deposit. This hypothesis seems to be validated also by the observation that the first phenomenon is smaller than the later one and this results also by the numerical simulation.

This sequence of events must be checked considering: i) different initial morphologies of the slopes; ii) the different nature of the two parts constituting the sliding surface: the tectonic discontinuity in the upper part and the bedding planes in the lower one; iii) the non uniform distribution of the shear resistance on the sliding surface, due to the different characteristics of these two parts and to the presence of rock bridges at the transition between them; iv) the presence of a realistic groundwater level in the rock mass.

The study is likely to better estimate possible future seismic landslides on the upper slope and run outs, that represents the major risk factor for the valley bottom villages: type of earthquake source and site conditions need to be, then, better understood both from field evidence and modeling.

REFERENCES

- BARBIERI G., CUCATO M., DEL PIERO W., DE ZANCHE V., GIANOLLA P., GRANDESSO P., MIETTO P., ROGGI G., SCHIAVON E., STEFANI C., VISONÀ D., ZAMPIERI D. & ZANFERRARI A. (2007) - *Note illustrative della Carta Geologica d'Italia alla scala 1:50.000 - Foglio 082 Asiago*. APAT-Servizio Geologico d'Italia, Regione del Veneto, 1-135, Firenze: S.EL.CA.
- BARTON N. & BANDIS S.C. (1990) - *Review of predictive capabilities of JRC-JCS model in engineering practice*. Proc. Int. Symp. on rock joints, Loen, Norway, 603–610.
- BHASIN R. & KAYNIA A.M. (2004) - *Static and dynamic simulation of a 700-m high rock slope in western Norway*. Engineering Geology, **71**: 213-226.
- BOUISSOU S., DARNAULT R., CHEMENDA A. & ROLLAND Y. (2012) - *Evolution of gravity-driven rock slope failure and associated fracturing: Geological analysis and numerical modelling*. Tectonophysics, 526–529.
- BOZZANO F., MARTINO S., NASO G., PRESTININZI A., ROMEO R.W. & SCARASCIA MUGNOZZA G. (2004) - *The large Salcito Landslide triggered by the 31st October 2002 Molise Earthquake*. Earthquake Spectra, **20**(2): 1-11.
- DAL PRÀ M. (1992) - *La frana di Casotto (VI): Studio geomeccanico ed analisi a ritroso con il metodo agli elementi finiti*. Unpublished Master thesis. Tutor: R. Genevois. University of Ferrara, Italy.
- DHAKAL S. (2004) - *Empirical relations for earthquake response of slopes*. PhD thesis, Institute for Geo-information Science and Earth Observation. Delft, The Netherlands.
- GERRARD C.M. (1982) - *Elastic models of rock masses having one, two and three sets of joints*. Int. J. Rock Mech. Min. Sci. & Geomech. Abstr., **19**: 15-23.
- GOODMAN R. E. (1976) - *Methods of geological engineering ion discontinuous rocks*. West, New York, 476 pp.
- GUIDOBONI E., COMASTRI A. & BOSCHI E. (2005) - *The 'exceptional' earthquake of 3 January 1117 in the Verona area (northern Italy): A critical time review and detection of two lost earthquakes (lower Germany and Tuscany)*. J. Geophys. Res., **110**, B12309: 1-20.
- HOEK E. (2007) - *Practical Rock Engineering*. www.rocksience.com
- INGV - ISTITUTO NAZIONALE DI GEOFISICA E VULCANOLOGIA (2007) - *Interactive Seismic Hazard Maps*.
- ITASCA. FLAC (2012) - *Fast Lagrangian analysis of continua, version 7.0*. Minneapolis: Itasca Consulting Group, Inc.
- ITASCA. UDEC (2011) - *Universal distinct element code, version 5*. Minneapolis: Itasca Consulting Group, Inc.
- IVERSON N. R. (2012) - *A theory of glacial quarrying for landscape evolution models*. Geology, **40** (8): 679-682.
- LORIG L.J., HART R.D. & CUNDALL P.A. (1991) - *Slope stability analysis of jointed rock using the distinct element method*. Transportation Research record 1330. TRB, National Research Council, Washington, DC, 1-9.
- MADDALENA L. (1906) - *Osservazioni geologiche sul vicentino ed in particolare sul bacino del Posina*. Boll.Soc.Geol.It., 25: 659-743.
- SERVA L. (1990) - *Il ruolo delle Scienze della Terra nelle analisi di sicurezza di un sito per alcune tipologie di impianti industriali: il terremoto di riferimento per il sito di Viadana (MN)*. Boll. Soc. Geol. It., **109**: 375-411.
- SINGH B. (1973a) - *Continuum characterization of jointed rock masses Part I- The constitutive equations*. Int. J. Rock Mech. Sci. & Geomech. Abstr., **10**: 311-335.
- SINGH B. (1973b) - *Continuum characterization of jointed rock masses Part II- Significance of low shear modulus*. Int. J. Rock Mech. Sci. & Geomech. Abstr., **10**: 337-349.
- ZAMPIERI D. & ADAMI S. (2013) - *Geological investigations on a potential rockslide impacting on a designed motorway in the Southern Alps (NE Italy)*. This volume.
- ZHANG C., PEKAU O.K., FENG, J. & GUANGLUN, W. (1997) - *Application of distinct element method in dynamic analysis of high rock slopes and blocky structures*. Soil Dyn. Earth. Eng., **16**: 385– 394.